A Pole Sharing Technique for Linear Phase Switched-Capacitor Filter Banks[1]

JOSEPH S. CHANG AND Y. C. TONG

Abstract —A switched-capacitor pole sharing technique for implementing bandpass filter banks is proposed. Using this technique, hardware reduction is achieved in two ways. First, the efficient nonminimum phase Lerner filter approximation is employed to minimize the number of poles required to satisfy a given filter specification in frequency and time domains; this approximation is more efficient than the common minimum phase filter approximations used in many reported filter bank designs. Second, the number of poles is reduced by pole sharing where an n-pole pair per channel bandpass filter bank is realized with only $(n-2)$ additional pole pairs per channel after the first channel, hence a saving of two pole pairs per channel. In the case of a four-pole pair (eighth order) per channel 25 channel filter bank example discussed in this paper, the number of poles saved is nearly 50%. The proposed hardware reduction methodology is micropower compatible, and is achieved without placing extra demands on the speed of operational amplifiers employed and without resorting to complicated clocking strategies; only a biphasic clock is used. Phase reversal for vocoder applications is easily achieved without incurring any additional hardware or compromising desirable features of the filter bank realization. Single parameter and statistical multiparameter sensitivity analyses are derived. The multiparameter sensitivity for the filter realized as a summation (parallel) of biquadratic sections is compared against the cascade structure.

A uniformly and nonuniformly spaced filter bank were simulated with SWITCAP and part of the uniformly spaced filter bank was constructed on a breadboard. The near linear phase in the passband and sharp attenuation in the stopband responses obtained agreed with filter specifications.

I. Introduction

SWITCHED-capacitor (SC) filters comprising operational amplifiers (op amps), capacitors, and switches have been widely used in the electronics industry in recent years. Its popularity is a consequence of its ease and precise implementation in monolithic form using current MOS large-scale integration processes. In particular, its transfer function is accurately realized as its transfer function coefficients are completely specified by the crystal-controlled clock frequency and precise (typically 0.1%) capacitors ratios. However, as the need for complex on-chip systems grow, chip area and power consumption remain major obstacles. An example of such a system is a filter bank for speech recognition [1]–[4], vocoders [5], spectrum analyzers, etc., where a large number of high order filters are used.

Techniques to alleviate the chip area and power dissipation problems in a filter bank include the use of micropower op amps, micropower compatible feedback networks in filter topologies [7], time-division-multiplexing [3], [5], and use the efficient filter approximations [6], [8], [9] in terms of the number of poles required to satisfy a given filter specification in frequency and time domains. Although time-division-multiplexing has been effectively employed to reduce total hardware as it permits sharing of op amps and capacitors between channels, its application suffers from several drawbacks. In an SC time-division-multiplexing scheme, op amps service different subcircuits in successive time slots (clock phase in local clock periods) in a periodic manner. Because of the reduced duration of these time slots compared to unmultiplexed circuits, higher speed op amps are required. Furthermore, a complex clocking circuitry is required to generate the many different clock signals. These costs would in turn compromise power dissipation and chip area, thus somewhat defeating the objectives in the first place.

This paper discusses a pole sharing technique using the non-minimum phase Lerner filter approximation for implementing a bandpass filter bank. This technique permits sharing of biquadratic filter sections, hence hardware savings, without placing additional speed requirements on the op amps employed and without resorting to complicated clocking strategies; only a biphasic clock is used. A pole shared *RLC* implementation was reported in the mid-sixties [10]. In this paper, the implementation is modernized to SC and several novel designs, including phase inversion without incurring additional hardware, switch and capacitor sharing, to further enhance the advantages offered by the pole sharing methodology are presented. The hardware savings achieved is significant, for example, nearly 50% reduction in the number of pole pairs for a four-pole pair (eighth order) per channel filter bank when compared to a conventional direct (unmultiplexed) implementation.

Manuscript received March 23, 1988; revised January 8, 1990. Part of this paper was presented at the 1988 IEEE International Symposium on Circuits and Systems, Helsinki, Finland. This work was supported by the Australian National Health and Medical Research Council, by the National Institutes of Health (USA) under Contract 1-NS-5-2388, by the Deafness Foundation (Victoria, Australia), and by the University of Melbourne Postgraduate Scholarship. This paper was recommended by Associate Editor J. Mavor.

The authors are with the Department of Otolaryngology, Human Communication Research Center, University of Melbourne, Parkville, Vic. 3052, Australia.

IEEE Log Number 9039216.

[1]Patent pending.

0098-4094/90/1200-1465$01.00

The modernized pole sharing methodology has several features worthy of mention. First, the efficient nonminimum phase Lerner filter approximation is employed; more efficient, in terms of the number of poles required to satisfy a given filter specification, than popular minimum phase approximations. Furthermore, use of the Lerner filter approximation results in bandpass filters that possess an arithmetically symmetrical magnitude response, a desirable frequency response [9], [11]. This is unlike usual bandpass filter designs derived from lowpass prototypes via impedance transformation [8], [11] where the magnitude response is geometrically symmetrical. Second, by pole sharing, the number of poles necessary for the synthesis of a bank of contiguous bandpass filters is reduced and consequently, a more economical and simplified design procedure. Thus the savings is simultaneously achieved in two ways.

Third, all feedback networks employed to realize the Lerner filter topology can easily be designed to be compatible with micropower by using uncoupled amplifier and coupled-in-cascade amplifier structures [7] only. In this paper, the term "micropower compatible" means that only these amplifier structures are employed. Fourth, with this pole sharing technique, the magnitude response of adjacent channels of a bandpass filter bank can easily be designed to overlap at the -3-dB point, a very desirable feature that yields an overall flat composite spectrum. In addition, design of the Lerner filter to approximate the specified magnitude and phase ripple responses by adjusting the transfer function parameters can easily be incorporated in a filter synthesis algorithm. Finally, in vocoder applications [6], it is desirable to invert the phase of some channels of a filter bank for improved performance. This phase inversion can be accomplished without incurring any additional hardware or compromising any features of the filter bank realization, in particular micropower compatibility and parasitic insensitivity (or parasitic compensated). The pole sharing methodology is also applicable to active *RC* realizations, continuous-time MOSFET-C filters, and digital filter implementations.

In this paper, subcircuits comprising biquadratic sections and summer/sample-and-hold circuits for the realization of the Lerner filter are presented. These subcircuits differ markedly from a recent SC Lerner filter realization [13]. In particular, micropower compatibility and parasitic insensitivity (or compensated) are strictly observed here. Designs to realize the full Lerner transfer function for general bandpass Lerner filter implementations, instead of its simplified function for speech analysis bandpass filter banks, are also presented in this paper. Single parameter and statistical multiparameter sensitivities are derived.

This paper is arranged in the following manner. Section II discusses the Lerner approximation for SC filters. Design considerations for appropriate biquadratic sections, summer/sample-and-hold circuits and the Lerner filter realization are discussed in Section III. Section IV presents the pole sharing technique and two filter bank

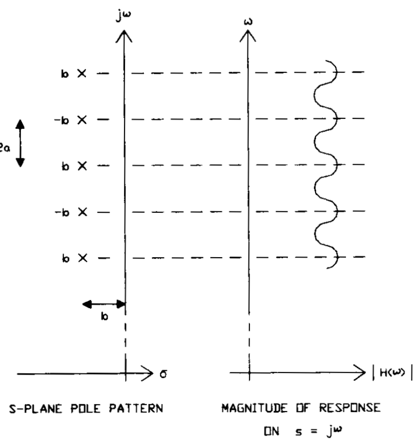

Fig. 1. Pole residue pattern and magnitude response of the Lerner function in the s-plane.

design examples are given in Section V. Sensitivity analyses are derived in Section VI. Single ended output op amps will only be employed in this paper to illustrate the pole sharing technique; extension to include differential output op amps is straightforward.

II. Lerner Filter Approximation

Filtering in frequency and time domains is well documented in literature [8], [11]. In many applications, a sharp attenuation and flat group delay are specified. Spectrum analyzers based on a filter bank configuration for automatic speech recognition and vocoders are some applications. In many speech analysis filter banks, minimum phase filter approximations [1]–[6], [11] with a linear phase characteristic are used to satisfy the time-domain requirements. These approximations are, however, inefficient in terms of the number of poles required to satisfy the attenuation specifications.

The Lerner filter function is a nonminimum phase approximation. Nonminimum phase approximations are more efficient than the popular minimum phase functions and hence reduced circuit complexity because the attenuation and phase responses of the minimum phase functions are restricted by a Hilbert transform pair for stability reasons [8], [9], [11]. The Lerner filter approximation is expressed as a summation of weighted poles in (1):

$$H(s) = \frac{r_1}{(s-p_1)} + \frac{r_2}{(s-p_2)} + \frac{r_3}{(s-p_3)} + \cdots + \frac{r_n}{(s-p_n)} \quad (1)$$

where r_n is the residue of $H(s)$ at the pole p_n.

The infinite Lerner function is given in (2) where it is noted that the pole separation along the $j\omega$ axis is $2a$ and the real part $-b$. The residues of the poles are of equal weight b but alternate in sign. Fig. 1 depicts the pole residue pattern and magnitude response on $s = j\omega$. Approximated expressions for the magnitude and phase of

$H(s)$ are given in (3).

$$H(s) = \sum_{k=-\infty}^{\infty} \left[\frac{b(-1)^k}{s - j2ka + b} \right] \tag{2}$$

$$|H(j\omega)| \approx (\pi bc/a)\left[1 + c^2 \cos(\pi\omega/a) + \cdots\right] \tag{3a}$$

$$\phi \approx -\left[\pi\omega/2a + c^2 \sin(\pi\omega/a) + \cdots\right] \tag{3b}$$

$$c = e^{-\pi b/2a}. \tag{3c}$$

Thus $H(j\omega)$ approximates a constant magnitude with a periodic ripple whose relative amplitude is c^2, and approximates a time delay of $\pi/2a$ seconds to within a maximum periodic error of c^2.

In a Lerner bandpass filter, the band edge is defined (by the designer) to be halfway between the frequencies of two consecutive poles of (2). Poles that are above and below the band edges are dropped and corrector poles added at the band edges to smooth the transition from passband to stopband. The bandpass Lerner function is now truncated and rearranged to (4) in order to utilize biquadratic sections as its "workhorse." The poles within the band edges are termed in-band poles and the attenuation at the corrector poles at the band edges is -6 dB.

$$\begin{aligned} H(s) = \Bigg[& \sum_{k=x_l}^{x_h} \frac{2b(s+b)(-1)^k}{s^2 + 2bs + \{2a(k+\alpha)\}^2 + b^2} \quad \text{in-band poles} \\ & + \left(\frac{b(s+b)(-1)^{x_l - 1}}{s^2 + 2bs + \{(2n_l - 1)a\}^2 + b^2} \right) \quad \text{low frequency corrector poles} \\ & + \left(\frac{b(s+b)(-1)^{x_h + 1}}{s^2 + 2bs + \{(2n_h + 1)a\}^2 + b^2} \right) \Bigg] \quad \text{high-frequency corrector poles} \end{aligned} \tag{4}$$

where

$x_h - x_l + 3$	number of pole pairs,	(5a)
$a[2(x_l + \alpha) - 1]$	imaginary part of lowest frequency corrector pole,	(5b)
$n_l =$	$(x_l + \alpha)$	(5c)
$n_h =$	$(x_h + \alpha)$.	(5d)

Also, α is a fraction and x_l, x_h integers. For an SC implementation, the Laplace to z-plane transformation chosen is the matched z transformation [13]. In this fashion, poles at equal intervals (except the corrector poles) along the $j\omega$ axis in the s-plane map to poles at equal intervals or angles in the z-domain as depicted in the pole plot in Fig. 2 for a five-pole pair bandpass Lerner filter. The z-domain truncated Lerner function is given in (6):

$$\begin{aligned} H(z) = \Bigg[& \sum_{k=x_l}^{x_h} \frac{2b(1 - z^{-1}e^{-aT})(-1)^k}{1 - 2z^{-1}e^{-bT}\cos\{2aT(k+\alpha)\} + e^{-2bT}z^{-2}} \quad \text{in-band poles} \\ & + \left(\frac{b(1 - z^{-1}e^{-aT})(-1)^{x_l - 1}}{1 - 2z^{-1}e^{-bT}\cos\{(2n_l - 1)aT\} + e^{-2bT}z^{-2}} \right) \quad \text{lowest frequency corrector poles} \\ & + \left(\frac{b(1 - z^{-1}e^{-aT})(-1)^{x_h + 1}}{1 - 2z^{-1}e^{-bT}\cos\{(2n_h + 1)aT\} + e^{-2bT}z^{-2}} \right) \Bigg] \quad \text{highest frequency corrector poles} \end{aligned} \tag{6}$$

where T is the sampling frequency^{-1}.

For a fixed number of poles, increasing the ratio b/a yields a slower cutoff filter, but a better approximation to linear phase in the passband and consequently, a less ringing impulse response. Adjustment of this parameter can be easily incorporated in a computer program to meet design specifications.

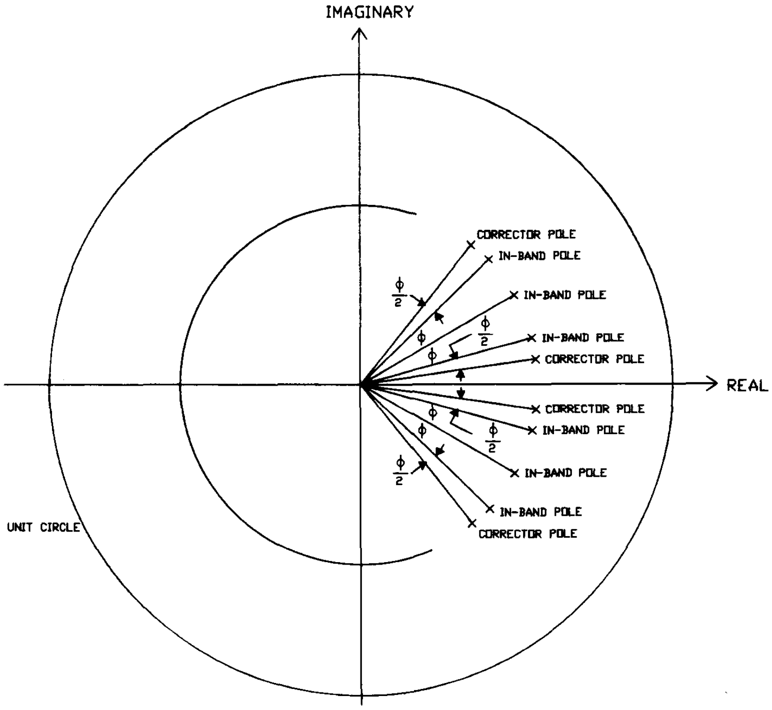

Fig. 2. Pole pattern of a truncated Lerner function in the z-plane for a five-pole pair bandpass filter.

It is possible to simplify the numerator of the biquadratic terms in (6) by placing a common first-order term at the outside of the square brackets as in (7). In typical speech analysis bandpass filter banks, the first-order term is ignored as it has negligible influence on the frequency response. This is further considered in the next section.

$$
\begin{aligned}
H(z) = \frac{2(1-z^{-1}e^{-aT})}{1-z^{-1}} \Bigg[& \sum_{k=x_l}^{x_h} \frac{b(1-z^{-1})(-1)^k}{1-2z^{-1}e^{-bT}\cos\{(2aTk+\alpha)\}+e^{-2bT}z^{-2}} \quad \text{in-band poles} \\
& + \left(\frac{(b/2)(1-z^{-1})(-1)^{x_l-1}}{1-2z^{-1}e^{-bT}\cos\{(2n_l-1)aT\}+e^{-2bT}z^{-2}} \right) \quad \text{lowest frequency corrector poles} \\
& + \left(\frac{(b/2)(1-z^{-1})(-1)^{x_h+1}}{1-2z^{-1}e^{-bT}\cos\{(2n_h+1)aT\}+e^{-2bT}z^{-2}} \right) \Bigg] \quad \text{highest frequency corrector poles}
\end{aligned} \tag{7}
$$

A recommended design methodology for bandpass Lerner filters (and filter banks) is as follows.

i) For a specified relative in-band magnitude ripple c^2 (eq. 3), determine ratio (b/a);

ii) For a specified in-band time delay ripple c^2 seconds (eq. 3), determine ratio (b/a);

iii) Subsequently, choose the larger (b/a) ratio to satisfy both magnitude and delay ripple specifications;

iv) For an initial estimate of the number of pole pairs, p ($p=4$ minimum), and given the bandwidth between band edges $\Delta_{6\,\mathrm{dB}}$, evaluate

$$y = 2p-4$$

and

$$a = \Delta_{6\,\mathrm{dB}}/y.$$

Hence determine b from step iii);

v) For the given lowest frequency bandedge ω_{b1}, the imaginary part of the lowest frequency corrector pole = ω_{b1}. From (5b), evaluate $(x_l+\alpha)$ using

$$(x_l+\alpha) = 1/2(\omega_{b1}/a+1).$$

Hence determine x_l as the integer and α as the fraction of the mixed number $(x_l+\alpha)$;

vi) Finally, determine x_h, n_l, and n_h, respectively, from (5a), (5c), and (5d). All the coefficients of (7) can now be computed;

vii) Evaluate $H(z)$ by substituting $z = e^{j\omega T}$ and if design specifications are not satisfied, one or more of the following may be considered: (a) Modify the b/a ratio; (b) Increase the number of pole pairs, and repeat steps iv to vii; (c) Adjust the Lerner approximation (e.g., see Section V and [9]) which leads to a slightly modified form of the Lerner transfer function; and

viii) Design the biquadratic sections and summer/sample-and-hold circuit (Section III).

III. Design Considerations

The block schematic diagram for the realization of a Lerner filter is depicted in Fig. 3(a). Consider first, the case where the first-order common term (eq. 7) is ignored. A circuit diagram of a Lerner filter is given in Fig. 3(b) (ignore the first-order circuit on the extreme right-hand side as indicated at the bottom of Fig. 3(b)). The realization involves a number of biquadratic sections connected in parallel whose outputs are sampled (and summed) by a summer/sample-and-hold circuit as required in the square brackets of (7). The clock signal used is the biphasic clock comprising non-overlapping even and odd phases, also depicted in Fig. 3.

A well designed biphasic biquadratic section should possess the following characteristics:

(a) parasitic insensitivity or compensated;
(b) stable by having its overall feedback loop "broken" in both phases, hence avoiding an active-C filter configuration at all times;
(c) easily gain scale outputs for maximum dynamic range;
(d) easily cascadable by providing a sample-and-hold output by designing the output op amp in a manner such that it samples the input only during one phase [14];
(e) possess low capacitor ratio spread;
(f) insensitive to component changes;
(g) compatible with micropower designs by limiting all feedback networks to uncoupled amplifier and coupled-in-cascade amplifier configurations.

Although criterion (d) is desirable primarily for cascading biquadratic filter sections in a high-order cascade synthesis, it is necessary here for two other reasons. First, the summer/sample-and-hold circuit is designed to sample (sample-and-hold) outputs of different biquadratic sections during the even and odd clock phases of the same clock period. This is shown in Fig. 3(b) where the C' capacitor of the summer/sample-and-hold circuit samples the output of two biquadratic sections and the sign inversion is performed as required in (7). This C' capacitor is shared by two biquads. Second, criterion (d) is required as a prerequisite to satisfy the micropower criterion (g) because the output op amp of the biquadratic section is not permitted to sample an input when its output is sampled by the op amp of the summer/sample-and-hold circuit. This is the case of the odd phase in Fig. 3(b).

Nine biquadratic sections employing single ended output op amps presented in [14] that meet the above-mentioned criteria and satisfy the second-order transfer functions in (7) are given in Fig. 4(a)–(i). Note that only six or less capacitor switch networks are used in these structures. A capacitor switch network is a capacitor and its associated switches. The appropriate choice of which of the nine biquadratic sections to use depends on performance criteria such as total capacitance, capacitance spread, dynamic range, sensitivity, power dissipation, etc. No general rules are available as the performance criterion depends on pole Q, gain constant, sampling rate, etc. One of the nine biquads, "PTF," will be used to illustrate the pole sharing technique in Section IV. Its signal-flow-graph [15] and transfer function are depicted in Fig. 4(a).

If the pole and zero of the first-order common term in (7) are close to the band edge of the Lerner filter, it may be necessary to realize the Lerner filter using the original configuration of the summation of biquadratic terms in (7). Suitable biquadratic sections that meet criteria (a)–(g) include the nine in Fig. 4 with minor changes to the capacitor switch networks in the feedforward path. Other suitable biquadratic sections include the "AUL", "AUV", "AAUV", "AUVV", "PTV", "PTTV", "PTVV", "PVV", "PFF", and "UVV" biquadratic sections given in [14]. Caution should be exercised in the selection of the feedforward capacitor switch networks to meet criteria (d) and (g) above. The above-mentioned biquadratic section structures for realizing the biquadratic terms in (6) require one additional capacitor switch network when compared to those in (7). This is because of the e^{-aT} term in the numerator of the biquadratic transfer function in (6). An alternative method to account for the first-order term is to realize both the first-order common term and biquadratic terms in (7) individually and cascading them. The first-order common term circuit realization is depicted in Fig. 5(d) which may be used in conjunction with the summer/sample-and-hold circuit depicted in Fig. 5(b) or (c). The Lerner filter implementation using this method is shown in Fig. 3(b) which also satisfies the micropower and parasitic insensitivity criteria. It is reiterated here that for typical speech analysis filtler banks, only the summation of the biquadratic terms in (7) need be realized and henceforth, this is the case considered.

The residues of the corrector and in-band poles correspond to the values of the C' and $2C'$ capacitors respectively as depicted in Fig. 3(b). Biquadratic sections 1 and 4 are corrector pole pairs, two and three in-band pole pairs.

Phase inversion desirable for some filter channels in vocoder applications [6] is accomplished by simply swapping the even and odd clock phases of the pair of input switches of the C' and $2C'$ capacitor switch networks of the summer/sample-and-hold circuit. No additional hardware is incurred for this phase inversion, unlike the case of active RC or continuous-time MOSFET-C implemen-

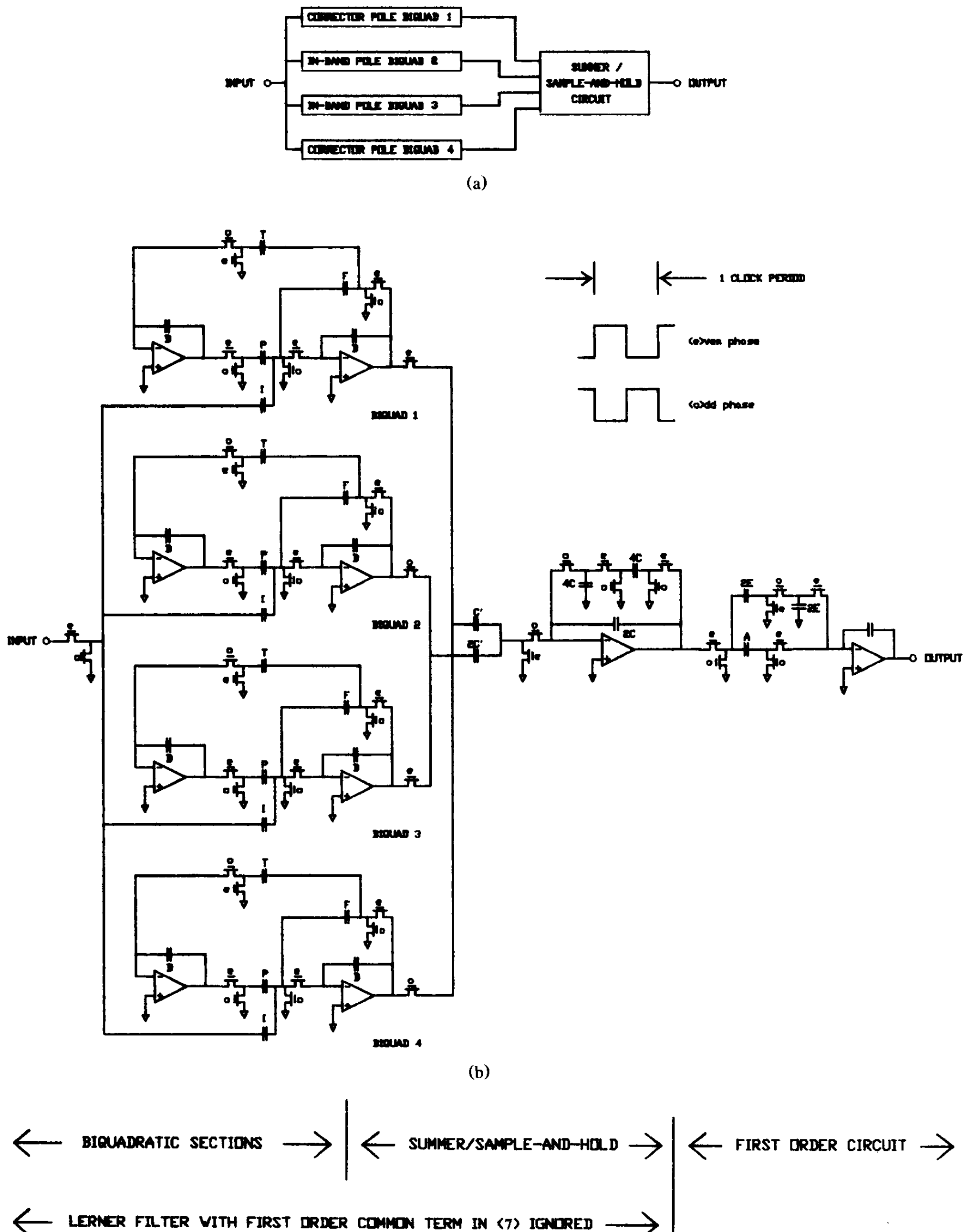

Fig. 3. (a) Schematic block diagram of a four-pole pair bandpass Lerner filter. (b) Circuit diagram of an eighth-order bandpass Lerner filter as expressed in (7).

tations employing single ended output op amps where an extra inverting amplifier is required. Furthermore, all desirable features of the Lerner filter are retained here.

The summation operation of (6) and (7) is realized by means of a summer/sample-and-hold circuit. Three summer/sample-and-hold circuits are given in Fig. 5(a)–(c), and their appropriate use depends on the output interface requirements of the Lerner filter. If the circuit of Fig. 5(a) is used, the output of the filter is available only during the odd phase. Thus this circuit is strictly a summer circuit as its output is not held for a complete clock period. The circuit in Fig. 5(b) provides a sample-and-hold

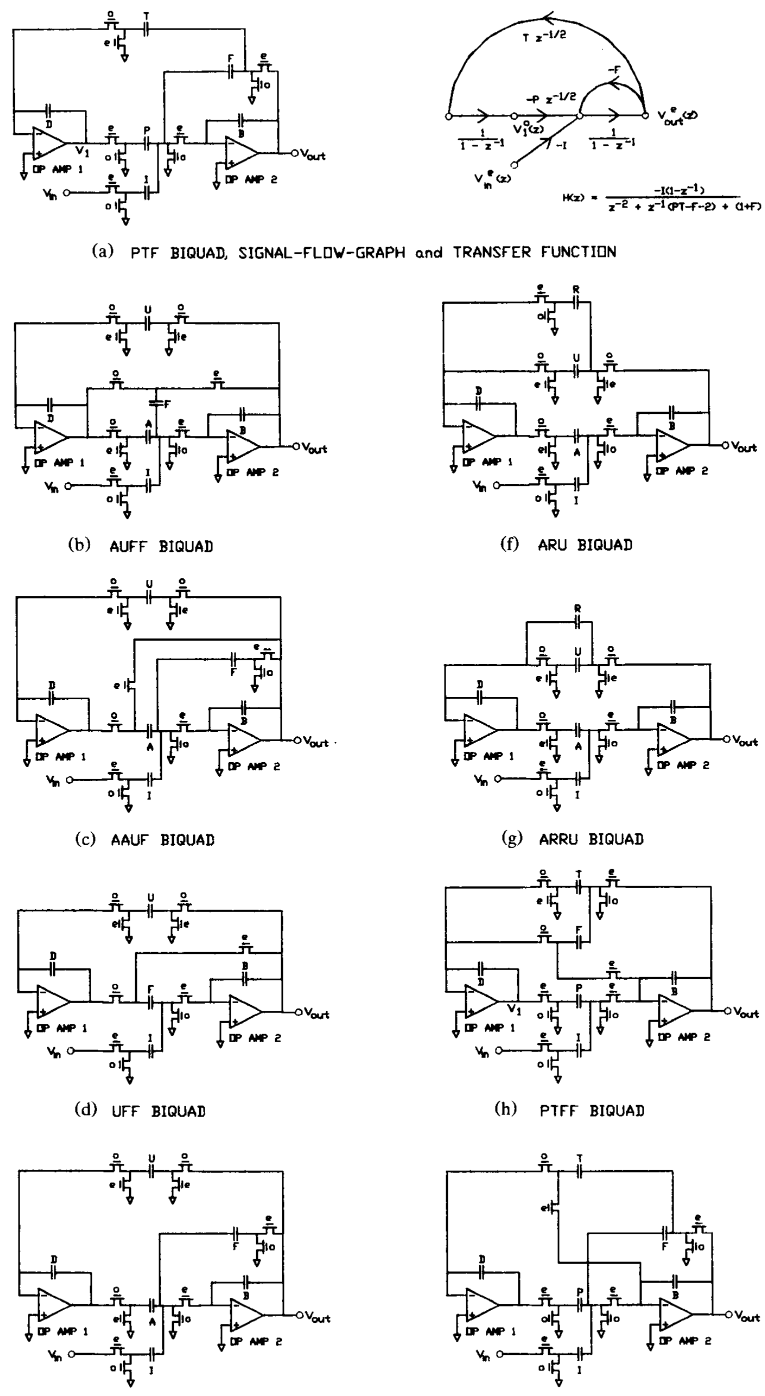

Fig. 4. (a) Circuit diagram, signal flow graph, and transfer function of the PTF biquadratic section. (b)–(i) Circuit diagram of other suitable biquadratic sections.

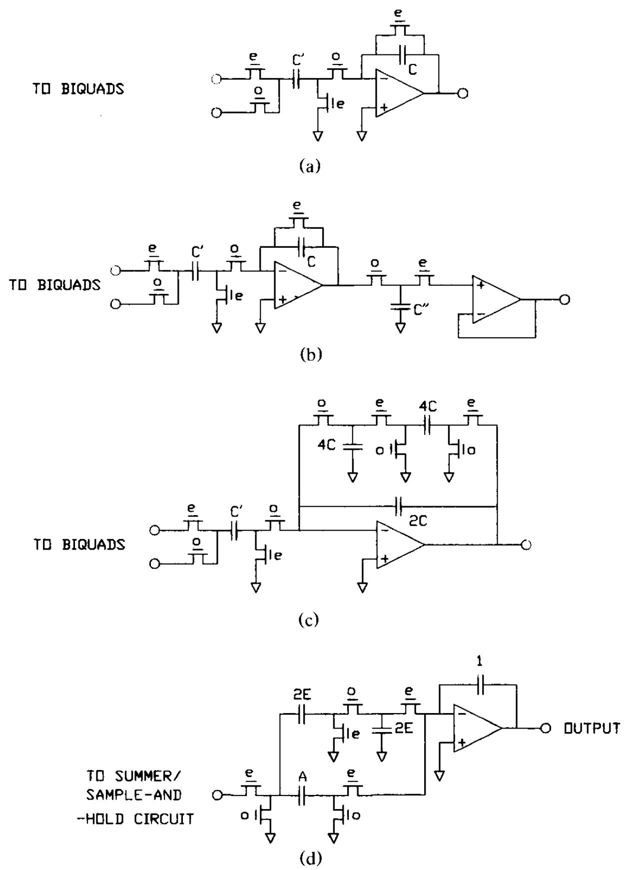

Fig. 5. (a)–(c) Circuit diagram of summer/sample-and-hold circuits. (d) First-order circuit to account for common first-order term in (6).

output at the cost of an additional op amp. This circuit may be more useful, for example, if the Lerner filter is interfaced to an A/D converter. The sample-and-hold output would alleviate the speed requirements of the following A/D. Employing circuit 5(c), as in this article, provides a sample-and-hold output without the cost of an additional op amp. It, however, uses an inverting parasitic compensated toggle switch [16] and hence the small cost of additional capacitors and careful layout at two nodes. These summer/sample-and-hold circuits are designed such that when they are used in conjunction with any of the biquadratic sections depicted in Fig. 4 for realizing a Lerner filter, the micropower compatibility and parasitic insensitivity criteria are observed. The summer/sample-and-hold circuits shown in Fig. 5(a)–(c) have inputs connected to the preceding biquadratic sections in a Lerner filter realization as indicated.

IV. Pole Sharing Technique

A direct result of the Lerner filter approximation expression as a summation of weighted poles is the parallel interconnection of the biquadratic sections. The signals between the biquadratic sections are, therefore, decoupled because the output of all biquadratic sections are not sampled by any other biquadratic sections. This is a desirable feature because the micropower compatibility criterion between the biquadratic sections are automatically satisfied. A further consequence of the parallel biquadratic section connection is that poles of two channels of a filter bank may be shared if they are on the same location in the frequency plane [10], [12]. This is the case for the poles of the extreme (band edge) pole pairs of two adjacent channels of a bandpass filter bank as depicted in Fig. 6 for channels M and $(M+1)$ in the Laplace plane. Thus, with exception of the first filter channel, each n pole pair filter channel may be realized with only $(n-2)$ pole pairs, a savings of two pole pairs per channel.

To appreciate the significance of the savings achieved by the pole sharing methodology, consider a four-pole pair (eighth order) per channel, sixteen-channel bandpass filter bank depicted in Fig. 7 which employs the 'PTF' biquadratic section and summer/sample-and-hold circuit of Fig. 5(c). This is a typical spectrum analyzer design for speech recognition [1]–[5]. A total of 34 biquadratic sections are employed compared against 64 (16 channels × 4

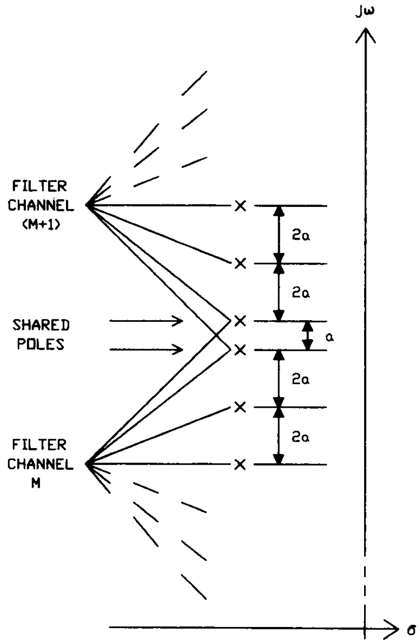

Fig. 6. Pole pattern depicting pole sharing in the s-plane for filter channels M and $(M+1)$.

biquads) required in a direct Lerner filter implementation. The biquadratic section savings achieved is thus nearly fifty percent in this case example. In addition, because the Lerner filter is an efficient approximation, in terms of the number of poles required to satisfy a given filter specification, the overall biquadratic section savings would exceed 50% compared to a more conventional high-order filter bank synthesis employing minimum phase filter approximations. Thus the considerable savings using the pole sharing Lerner filter methodology is achieved in two ways.

The overlap of the magnitude responses of adjacent filter channels depends on the b/a ratio since the magnitude and phase ripple responses are related to this ratio as expressed in (3). In the authors' experience, a typical b/a ratio between 1.5 and 2 would yield a good approximation to linear phase in the filter passband and a magnitude response overlap of approximately -2.7 dB between adjacent channels.

This magnitude overlap between channels suffices in most filter bank applications as the roll off beyond this point is sharp. A b/a ratio below and above the values of 1.5 and 2 usually yield an overlap less than -2.7 dB. However, if a precise -3-dB overlap (or other specified value), or a b/a ratio below 1.5 or above 2 is desired, the location of the in-band pole pair nearest the band edge and corrector pole pair at the band edge may be slightly adjusted to yield the appropriate filter responses. This will cause the filter response to deviate slightly from the Lerner approximation near the band edges as in the numerical example below.

V. Numerical Examples

Two pole-shared bandpass filter bank examples, uniformly and nonuniformly spaced center frequency filter banks, are designed in this section. First consider a uniformly spaced filter bank for speech applications with the following specifications:

i) four-pole pair per channel;
ii) 25 channels, uniform spacing;
iii) 120 Hz, -3 dB passbands for all channels: Channel (Ch) 1:300–420 Hz, Ch 2:420–540 Hz,$\cdots$,Ch 25:3180–3300 Hz;
iv) a:40 Hz, b:60, $b/a = 1.5$;
v) Sampling frequency: 20 kHz.

Using the filter design methodology in Section II resulted in magnitude responses of adjacent filter channels overlapping at -2.7 dB. To satisfy an overlap specification at -3 dB (specification iii), the in-band pole pair nearest the band edge and corrector pole pair at the band edge are moved towards each other by 2 Hz as tabulated in Table I for Ch 3–5. It can be seen from this table that two-pole pairs of adjacent channels are identically located and hence, they may be shared. By adopting the pole sharing technique, the number of biquadratic sections required is 52 compared to 100 using a direct (unshared) implementation.

With the first-order common term ignored in (7), and matching the coefficients of (7) with that of the "PTF" biquadratic section transfer function in Fig. 4(a), and finally performing dynamic range and capacitor scaling, the capacitor values are determined. These are shown in Table II for Ch 3–5.

Fig. 8 depicts the filter bank frequency response obtained by SWITCAP [19] computer simulations. A discrete realization comprising Ch 3–5 was constructed on a breadboard where capacitors used were within 2% of their designed values. Breadboard measured results agreed well with computer simulations. In particular, a good approximation to linear phase in the passband and sharp attenuation in the stopband were evident. In computer simulations, the magnitude overlap between adjacent channels were precisely at -3 dB and within ± 0.1 dB in breadboard measurements.

In some speech applications, the bandpass filters are spaced nonuniformly [1]–[5] whereby the passband bandwidth increases with increasing frequency. This spacing, often called "critical band spacing," corresponds to the frequency resolution of the human ear. Consider the following nonuniformly spaced filter bank specification:

i) four-pole pairs per channel;
ii) 16 channels, nonuniformly spacing;
iii) -3-dB bandwidths: Ch 1–9:120 Hz, Ch 10–16 increasing by a factor of 1.24
-3-dB passbands: Ch 1:300–420 Hz, Ch 2:420–540 Hz ,$\cdots$, Ch 16:2860–3300 Hz;
iv) b: 135, a ranges from 40 Hz (Ch 1)–146 Hz (Ch 16), b/a ranges from 3.4 (Ch 1)–0.92 (Ch 16);
v) Sampling frequency: 20 kHz.

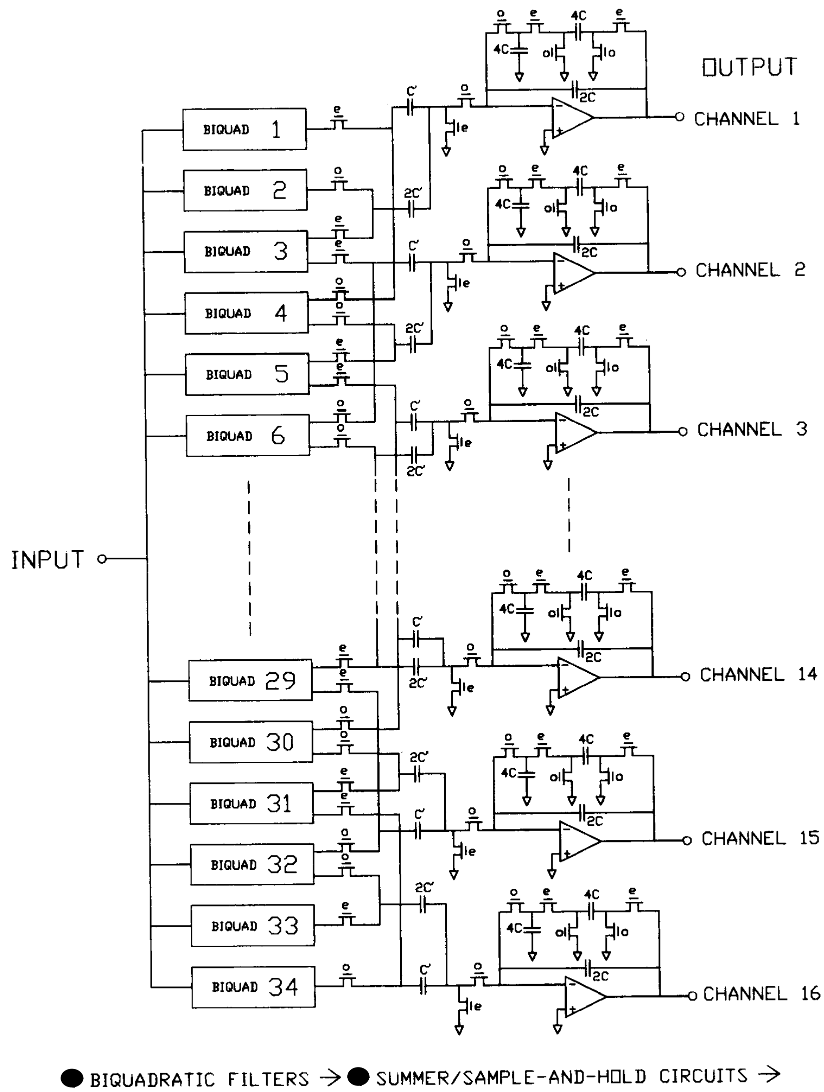

Fig. 7. Functional schematic of a four-pole pair per channel, sixteen channel filter bank embodying the pole sharing methodology.

TABLE I
LOCATION OF ADJUSTED IN-BAND AND CORRECTOR POLE PAIRS OF UNIFORMLY SPACED FILTER BANK

Channel	Low Freq Corrector	1st In-Band	2nd In-Band	High Freq Corrector
3	522 Hz	558 Hz	642 Hz	678 Hz
4	642 Hz	678 Hz	762 Hz	798 Hz
5	762 Hz	798 Hz	882 Hz	918 Hz

The derivation of the coefficients of (7) for Ch 1–9 were derived using the design methodology in Section II. However, as the center frequencies of Ch 10–16 are spaced nonuniformly, their pole locations were not located appropriately to permit pole sharing. A modification to the Lerner approximation can, however, be made. The method used here was to design the in-band pole pairs of a filter bank channel according to the Lerner approximation and use the nearest in-band pole pairs of both adjacent channels as its corrector pole pairs. In this manner, the corrector pole pairs of Ch 10–16 (and highest frequency corrector pole pair of Ch 9) were obtained. Other methods may be used, for example, the corrector and its nearest in-band pole pairs of one filter bank channel may be placed at the midpoint of the position obtained from the Lerner approximation and that of the adjacent channel (which is also derived from the Lerner approximation). Such pole pair positions may serve as initial estimates and subsequently adjusted in computer-aided designs.

Fig. 9 depicts the frequency response of the nonuniformly spaced bandpass filter bank using SWITCAP. A good approximation to linear phase and a fairly sharp

TABLE II
CAPACITOR (CAP) VALUES OF THE THREE UNIFORMLY SPACED FILTER BANK CHANNELS AFTER DYNAMIC RANGE AND CAPACITOR SCALING

Channel 3

Biquad	Cap B	Cap D	Cap F	Cap I	Cap P	Cap T
1	26.110	6.096	1.003	1.000	4.413	1.000
2	26.110	5.711	1.003	1.000	4.707	1.000
3	26.110	4.969	1.003	1.000	5.402	1.000
4	26.110	4.706	1.003	1.000	5.704	1.000

Summer/Sample-and-Hold C' : 1.101; C : 1.000

Channel 4

Biquad	Cap B	Cap D	Cap F	Cap I	Cap P	Cap T
1+	26.110	4.969	1.003	1.000	5.402	1.000
2+	26.110	4.706	1.003	1.000	5.704	1.000
3	26.178	4.183	1.006	1.000	6.386	1.000
4	26.178	3.997	1.006	1.000	6.686	1.000

Summer/Sample-and-Hold C' : 1.101; C : 1.000

Channel 5

Biquad	Cap B	Cap D	Cap F	Cap I	Cap P	Cap T
1+	26.178	4.183	1.006	1.000	6.386	1.000
2+	26.178	3.997	1.006	1.000	6.686	1.000
3	26.178	3.622	1.006	1.000	7.407	1.000
4	26.178	3.484	1.006	1.000	7.707	1.000

Summer/Sample-and-Hold C' : 1.101; C : 1.000

Biquadratic section (Biquad) 1 : Low frequency Corrector Pole Pair (Band edge)

Biquadratic section 2 : Low frequency In-Band Pole Pair

Biquadratic section 3 : High frequency In-Band Pole Pair

Biquadratic section 4 : High Frequency Corrector Pole (Band edge)

+ : denotes ***Pole Shared***

attenuation are evident. Ch 16 possessed the worst-case passband magnitude ripple of 0.5 dB (as evaluated in (3)) since its b/a ratio is smallest (specification (iv) above). The magnitude overlap between adjacent channels is between -2 and -3 dB and is satisfactory for most speech applications.

VI. SENSITIVITY

An important characteristic of a network function is the sensitivity of that function to parameter changes. In this section, single parameter sensitivity is derived in the s-plane and can easily be extended to the z-plane. The statistical multiparameter sensitivity is also derived and applicable to both s and z planes.

First consider the single parameter sensitivity S_x^H defined as

$$\Delta H/H = S_x^H(\Delta x/x) \tag{8}$$

where the changes in transfer function ΔH is related to the variations in parameter x. The operator, s, is dropped for brevity, e.g., $H(s)$ to H. Consider the infinite Lerner function (2) rewritten as

$$H = \sum_{k=-\infty}^{\infty}\left[\frac{r_k(-1)^k}{s - j\omega_k + b_k}\right].$$

The nominal values of b_k and r_k are b, and ω_k equal to $2ka$. In [9], it was shown that typical sensitivity values can be estimated by setting $k=0$ as $\omega_0 = 0$ represents one of the nominal pole positions. Sensitivity related to variations in parameter r_k, the residue, was shown to be

$$S_{r_k}^H = \frac{1}{H}\frac{b}{s+b}, \qquad \text{for } k=0 \tag{9a}$$

and sensitivity related to variations in the imaginary part of the pole location, ω_k, was shown to be

$$S_{\omega_k}^H = \frac{1}{H}\frac{a}{b}\frac{b^2}{(s+b)^2}, \qquad \text{for } k=0. \tag{9b}$$

By using (3), these sensitivities for an infinite Lerner transfer function can be rewritten as

$$S_{r_k}^H \approx \frac{a}{\pi bc}\left[\frac{b^2\cos\Psi - b\omega\sin\Psi}{b^2+\omega^2} - j\frac{b\omega\cos\Psi + b^2\sin\Psi}{b^2+\omega^2}\right] \tag{10a}$$

$$S_{\omega_k}^H \approx \frac{a}{\pi bc}\frac{a}{b}\left[\frac{b^2\{(b^2-\omega^2)\cos\Psi - 2b\omega\sin\Psi\}}{(b^2-\omega^2)^2+4b^2\omega^2} - j\frac{b^2\{(b^2-\omega^2)\sin\Psi + 2b\omega\sin\Psi\}}{(b^2-\omega^2)^2+4b^2\omega^2}\right] \tag{10b}$$

where $\Psi = \omega\pi/2a$ and ω is the difference between an oscillator test frequency and the nominal frequency of the pole. As the transfer function can be expressed as $H = |H|e^{j\phi}$, the single parameter magnitude and phase sensitivities are given by the real and imaginary parts of (10), respectively. Of particular interest, for the ratio of $b/a = 1.5$ (see filter bank example in Section V),

$$S_{r_k}^{|H|} \approx 2.2$$

$$S_{\omega_k}^{|H|} \approx 1.5$$

at the nominal pole frequency and these two sensitivities decrease to zero as a function of $1/\omega$ and $1/\omega^2$, respectively. On this basis, it can be remarked that the errors of a given pole are primarily confined to the vicinity of that pole and their effect on the magnitude transfer function is approximately two times as great as the parameter variation itself.

The single parameter sensitivity is a measure of the change in filter characteristic to a single parameter variation. It is important to identify the most sensitive parameter which has the largest sensitivity value. In a practical circuit, however, many parameters are varying simultaneously and a more acceptable figure-of-merit sensitivity measure is the statistical multiparameter sensitivity [17]. This sensitivity analysis takes into account multiparameter variations, considers the correlation between different parameters, and gives good agreement with Monte Carlo analysis. The multiparameter sensitivity analyses for the summation (parallel) of biquadratic section configuration H_L (Sections II and III) and cascade structure H_C are derived in Appendixes I and II. The frequency dependent integrand sensitivities, S_{T_L} and S_{T_C} for these N bi-

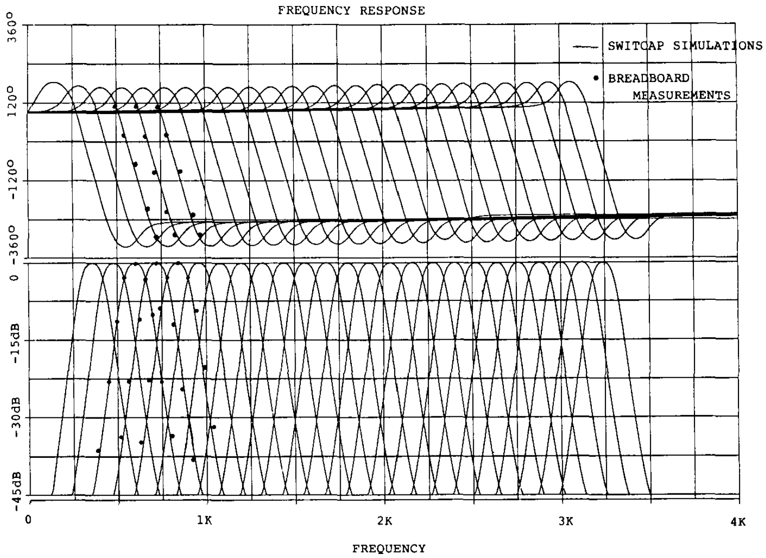

Fig. 8. Magnitude and phase response of uniformly spaced filter bank employing the pole sharing methodology obtained from SWITCAP computer simulations and discrete breadboard realization.

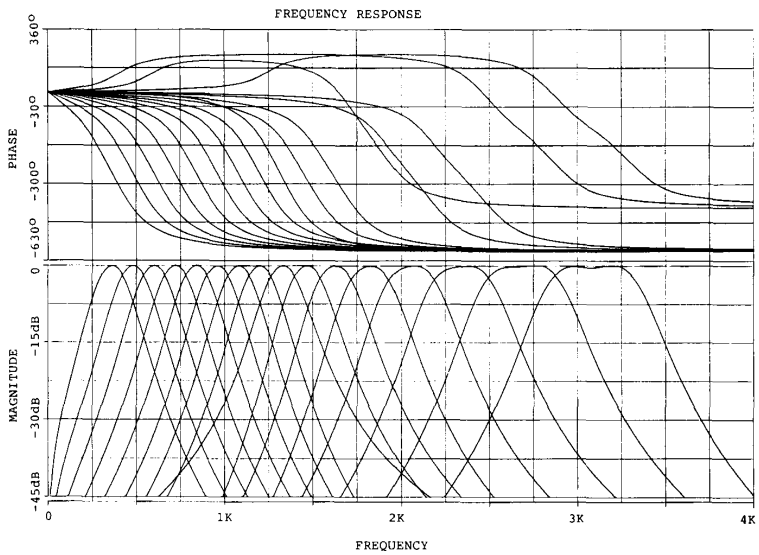

Fig. 9. Magnitude and phase response of nonuniformly spaced filter bank employing the pole sharing methodology obtained from SWITCAP computer simulations.

quadratic section structures are, respectively, given by

$$S_{T_L} = \frac{1}{|H_L|^2} \sum_{j=1}^{N} \left|T_j(H_L - T_j)\right|^2 S_{T_j} \tag{11}$$

$$S_{T_C} = \sum_{k=1}^{N} S_{T_k} \tag{12}$$

where T_j's are biquadratic sections of H_L, S_{T_j} and S_{T_k} are the frequency-dependent integrand sensitivities of the biquadratic sections of H_L and H_C, respectively. The sensitivities of these two filter realization structures can now be compared. It is first observed that for the same transfer function, the denominators of H_L and H_C are identical. In addition, in the case of high $Q (Q > 10)$ filters, the roots of the numerators of the H_L and H_C biquadratic sections are not close to those of the denominators of H_L (or H_C) and the influence of the numerator parameter variations on the frequency response in the passband is small. The variations of the numerator parameters can therefore be neglected [17] in the computation S_{T_j} and S_{T_k} and hence S_{T_j} and S_{T_k} can be treated as equal (eq. (A6)). Thus by comparing (A5) and (B2), the statistical multiparameter sensitivity of high Q filters real-

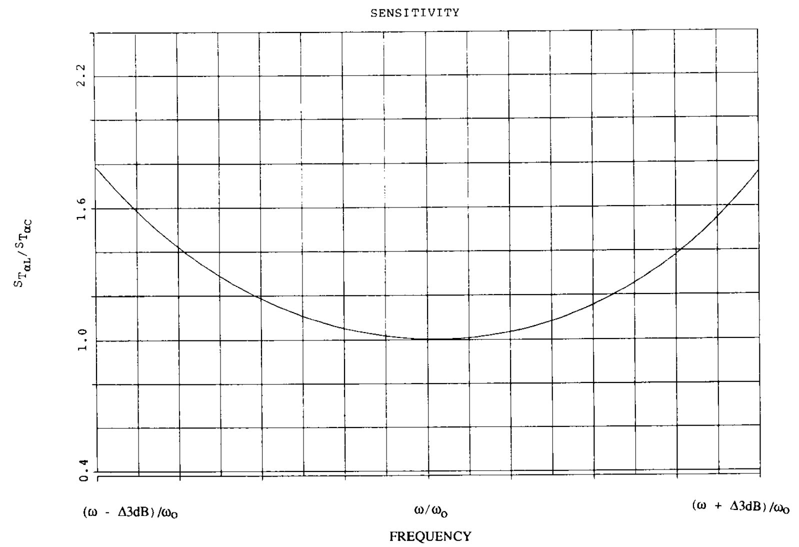

Fig. 10. Frequency-dependent integrand magnitude sensitivity ratio, $S_{T_{\alpha L}}/S_{T_{\alpha C}}$, comparing the summation of biquadratic section configuration H_L and cascade structure H_C.

ized by the H_L configuration is more sensitive than the H_C structure at frequencies where

$$S_{T_L} > S_{T_C}$$

or

$$\frac{1}{|H_L|^2} \sum_{j=1}^{N} \left| T_j(H_L - T_j) \right|^2 > 1 \tag{13}$$

and in the case of multiparameter magnitude sensitivity, S_{T_α}, and phase sensitivity, S_{T_β},

$$S_{T_{\alpha L}} > S_{T_{\alpha C}}$$

or

$$\sum_{j=1}^{N} \left[\mathrm{Re}\left(\frac{T_j(H_L - T_j)}{H_L} \right) \right]^2 > 1 \tag{14a}$$

$$S_{T_{\beta L}} > S_{T_{\beta C}}$$

or

$$\sum_{j=1}^{N} \left[\mathrm{Im}\left(\frac{T_j(H_L - T_j)}{H_L} \right) \right]^2 > 1 \tag{14b}$$

where Re denotes real and Im the imaginary parts, respectively.

As an example, consider the sensitivity of a high Q ($Q = 27$), four-pole pair bandpass Lerner filter used to realize channel 25 of a uniformly spaced filter bank (Section V). In this example, the assumption that the numerators of the biquadratic sections of H_L and H_C are far away from the roots of the denominator can be shown to be true. Fig. 10 depicts the frequency dependent integrand magnitude sensitivity ratio $S_{T_{jL}}/S_{T_{\alpha C}}$ against ω/ω_0; the range ω/ω_0 corresponds approximately to the -3-dB passbands bandwidths (note that in determining this sensitivity ratio, S_{T_j} and S_{T_κ} need not be computed). The ratio of $S_{T_{\alpha L}}/S_{T_{\alpha C}}$ is 1 at the center frequency and increases to 1.8 at the -3-dB passband. Hence, the magnitude sensitivity of the summation of biquadratic section configuration H_L is equal to the cascade structure H_C at the center frequency and slightly worse off at the -3-dB passband edge. The sensitivity of H_L is not expected to be a problem in most designs because the frequency-dependent integrand sensitivities of their biquadratic sections, S_{T_j} in (11), are usually small as the transfer function of SC circuits is determined by a crystal-controlled oscillator and precise capacitor ratios.

To compute S_{T_j} and S_{T_k} of high Q filters in (11) and (12), the single parameter sensitivity $S_x^{\omega_0}$ (where ω_0 is the center frequency), as shown in (A6), is required. In the derivation of the z-domain SC Lerner filter approximation from the Laplace plane, the matched z transformation was used. For this Laplace-to-z domain transformation, the biquadratic section $S_x^{\omega_0}$ sensitivity has been reported elsewhere [18] (poles of impulse invariant transformation are identical to matched z).

To summarize the sensitivity analysis, the single parameter sensitivity analysis demonstrated that the errors of a given pole are primarily confined to the vicinity of that pole. Furthermore, the multiparameter analysis demonstrated that for a high Q filter, the multiparameter magnitude sensitivity for the summation of biquadratic section filter configuration is only slightly worse off than the cascade filter structure in the vicinity of the poles (within the passband).

VII. Conclusions

A pole sharing technique for implementing bandpass filter banks using the efficient nonminimum phase Lerner approximation without placing additional speed requirements on the operational amplifiers and without resorting to complicated clocking strategies has been discussed; only a biphasic clock was used. Substantial hardware saving has been achieved. The filter synthesis was shown to be micropower compatible, parasitic insensitive, and phase reversal was easily accommodated while retaining all desirable features. A uniformly and nonuniformly spaced filter bank for typical speech applications have been simulated with SWITCAP and three channels of the uniformly spaced filter bank have been constructed on a breadboard using discrete components. The results obtained agreed with design specifications, yielding a good approximation to linear phase in the passband and sharp attenuation in the stopband. Single parameter and statistical multiparameter sensitivity analyses have been derived.

Appendix I

The statistical multiparameter sensitivity [17] measure is defined as

$$E\left[\int_{\omega_1}^{\omega_2}|\Delta H/H|^2\,d\omega\right]=\int_{\omega_1}^{\omega_2}S_T\,d\omega\approx\int_{\omega_1}^{\omega_2}\boldsymbol{d}_T^{t*}\boldsymbol{P}\boldsymbol{d}_T\,d\omega \quad \text{(A1)}$$

where S_T denotes the frequency dependent integrand sensitivity, t means transpose, E is the mathematical expectation, and ω_1 to ω_2 the frequency range of interest (usually passband). The covariance matrix $\boldsymbol{P}=E[\Delta x\,\Delta x^t]$ is of order $k\times k$, * denotes complex conjugate, and boldface denotes a vector. A typical component of $\boldsymbol{d}_T$ is

$$(d_T)_{x_i}=\frac{x_i}{H}\frac{\partial H}{\partial x_i}=S_{x_i}^H \quad \text{(A2)}$$

where x_i is a parameter of the filter transfer function H.

For the filter H_L realized as a summation (parallel) of N biquadratic sections T_j, $j=1,\cdots,N$,

$$H_L=\sum_{j=1}^{N}T_j \quad \text{(A3)}$$

it can be shown that

$$(d_T)_{x_i}=\frac{1}{H_L}\sum_{j=1}^{N}(H_L-T_j)T_jS_{x_i}^{T}. \quad \text{(A4)}$$

An assumption now taken is that the multiparameter variations within one biquadratic section are independent of the other biquadratic sections. This assumption is justified in a practical circuit if the biquadratic sections do not share components and the biquadratic sections are widely apart in an integrated circuit. Hence, the biquadratic sections are uncorrelated, i.e., covariance matrix

$$\boldsymbol{P}=\begin{bmatrix}P_1 & 0 & . & . & 0\\ 0 & . & & & .\\ . & & . & & .\\ . & & & . & 0\\ 0 & . & . & 0 & P_N\end{bmatrix}.$$

Thus

$$S_{T_L}=\frac{1}{|H_L|^2}\sum_{j=1}^{N}\left|T_j(H_L-T_j)\right|^2\boldsymbol{d}_{T_j}^{t*}\boldsymbol{P}_j\boldsymbol{d}_{T_j}$$
$$=\frac{1}{|H_L|^2}\sum_{j=1}^{N}\left|T_j(H_L-T_j)\right|^2S_{T_j} \quad \text{(A5)}$$

where

$$S_{T_j}=\boldsymbol{d}_{T_j}^{t*}\boldsymbol{P}_j\boldsymbol{d}_{T_j}$$
$$\boldsymbol{d}_{T_j}^{t}=S_{x_j}^{T_j}.$$

In the case of a high $Q(Q>10)$ filter, the roots of the numerators of T_j are not close to denominator of H_L and the influence of the numerator parameter variations on the frequency response in the passband is small. It can then be shown that the frequency dependent integrand sensitivity for biquadratic section T_j is

$$S_{T_j}\approx 4\omega_0^2\frac{1}{|D_j|^2}\sum_{u=1}^{m}\sum_{v=1}^{m}S_{x_u}^{\omega_0}S_{x_v}^{\omega_0}p_{uv} \quad \text{(A6)}$$

where D_j is the denominator of biquadratic section T_j and p_{uv} is the ith row, jth column of $\boldsymbol{P}$, and there are m parameters in T_j.

Appendix II

Consider now the statistical multiparameter sensitivity of an N biquadratic section cascade configuration whose transfer function is given by

$$H_C=\prod_{k=1}^{N}T_k.$$

Assuming that the multiparameter variations within one biquadratic section are uncorrelated to other biquadratic sections as in Appendix I, it can be shown that

$$S_{T_C}=\sum_{k=1}^{N}S_{T_k} \quad \text{(B1)}$$

and for high Q ($Q>10$) filters,

$$S_{T_C}\approx\sum_{k=1}^{N}S_{T_k} \quad \text{(B2)}$$

where S_{T_k} is frequency dependent integrand sensitivity of the biquadratic section T_k (in place of T_j) given in (A6).

Acknowledgment

The authors gratefully acknowledge the encouragement and support of Prof. G. M. Clark, and other staff members of the Department of Otolaryngology for useful discussions.

References

[1] Y. C. Tong, J. S. Chang, and J. M. Harrison, "Speech processors for auditory prosthesis," Quart. Prog. Rep. 1986–1988, National Institutes of Health (USA) Contract 1-NS-5-2388.

[2] ——, "Two speech processing schemes for the University of Melbourne multichannel cochlear implant prosthesis," in *Proc. IEEE Int. Symp. Circuits Syst.*, Portland, OR, pp. 1051–1054, 1989.

[3] Y. Kuraishi, K. Nakayama, K. Miyadera, and T. Okamura, "A single-chip 20 channel speech spectrum analyzer using a multiplexed SC filter bank," *IEEE J. Solid-State Circuits*, vol. SC-19, pp. 964–970, 1984.

[4] B. A. Dautrich, L. R. Rabiner, and T. B. Martin, "On effects of varying filter bank parameters on isolated word recognition," *IEEE Trans. Acoust., Speech, Signal Processing*, vol. ASSP-31, pp. 793–807, 1983.

[5] J. S. Chang and Y. C. Tong, "A low power time-multiplexed switched capacitor spectrum analyzer," in *Proc. Symp. VLSI Circuits*, Kyoto, Japan, pp. 91–92, 1989.

[6] R. M. Golden, "Vocoder filter design: Practical considerations," *J. Acoust. Soc. Amer.*, vol. 43, no. 4, pp. 803–810, 1967.

[7] P. M. V. Peteghem and W. M. C. Sansen, "Power consumption versus filter topology in SC filters," *IEEE J. Solid-State Circuits*, vol. SC-21, pp. 40–47, 1986.

[8] P. A. Kirton, "Linear phase and stripline filters," Ph.D. dissertation, Monash Univ., Australia, 1980.

[9] M. Lerner, "Band-pass filters with linear phase," *Proc. IEEE*, Vol. 52, pp. 249–268, 1964.

[10] P. R. Drouilett Jr. and L. M. Goodman, "Pole-shared linear-phase band-pass filter bank," *Proc. IEEE*, Vol. 54, pp. 701–703, 1966.

[11] H. J. Blinchikoff and A. I. Zverev, *Filtering in the Time and Frequency Domains.* New York, Wiley, 1976.

[12] J. S. Chang and Y. C. Tong, "A time-division-multiplexed pole sharing methodology for switched capacitor filter banks," in *Proc. IEEE Int. Symp. Circuits Systs.*, Helsinki, Finland, pp. 1245–1248, 1988.

[13] A. C. Lish, "A *z*-plane Lerner switched capacitor filter," *IEEE J. Solid-State Circuits*, vol. SC-19, pp. 888–892, 1984.

[14] J. C. M. Bermudez and B. B. Bhattacharyya, "A systematic procedure for generation and design of parasitic insensitive SC biquads," *IEEE Trans. Circuits Syst.*, vol. CAS-32, pp. 767–783, 1985.

[15] J. S. Chang, "A simplified signal-flow-graph approach to switched-capacitor analysis," *IREECON Tech. Dig. Papers*, pp. 895–898, 1987.

[16] K. R. Laker, P. E. Fleischer, and A. Ganesan, "Parasitic insensitive, biphasic switched capacitor filters realized with one op amp per pole pair," *Bell Syst. Tech. J.*, vol. 61, pp. 685–707, 1982.

[17] C. Acar and M. S. Ghausi, "A statistical multiparameter sensitivity measure of gain and phase functions," *Int. J. Circuit Theory Appl.*, vol. 5, pp. 13–22, 1977.

[18] D. E. Hocevar and W. K. Jenkins, "Sensitivity analysis of switched capacitor circuits," in *23rd MidWest Symp. Circuits Syst.*, Toledo, OH, pp. 439–443, 1980.

[19] S. C. Fang, Y. P. Tsividis, and O. Wing, "SWITCAP: A switched capacitor network analysis program," *IEEE Circuits Syst. Mag.*, Sept. Dec. 1983.

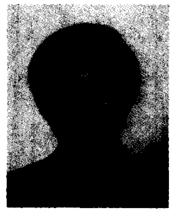

Joseph Chang received the B.E. degree in 1983 from Monash University, Australia, and the Ph.D. degree at the Department of Otolaryngology, University of Melbourne, in 1990.

He was awarded the first prize at the State and National levels in Mathematics in 1977, a commendation for Best Presentation of a Paper award in 1989, and the University of Melbourne Postgraduate scholarship from 1986–1989. He holds several patents in circuit design. His industrial experience include working for CSIRO and Texas Instruments in 1983–1985. He is presently a senior research scientist at the Human Communications Research Centre working in a multidisciplinary field, and a consultant to several hearing centers. He has been invited to give presentations at several conferences and workshops, and is a guest lecturer at several universities in Australia.

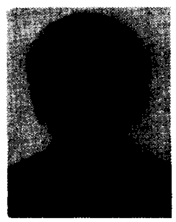

Y. C. Tong received the B.E. and Ph.D. degrees from the University of Melbourne, in 1972 and 1978, respectively.

Since 1976, he has been employed by the National Health and Medical Research Council of Australia (NH&MRC) to conduct research on communication aids for the hearing impaired at the Department of Otolaryngology, University of Melbourne. He is currently a Principal Research Fellow of NH&MRC. His research interests include auditory physiology, biophysics, signal processing, psychophysics, speech perception, biomedical engineering, and cochlear implant research. He is a co-inventor of several patents in cochlear implant and switched capacitor filter design. He is also the co-ordinator and senior investigator of a NIH (National Institutes of Health, USA) research grant and a NIH research contract for cochlear implant research at the University of Melbourne.